The British Journal of Radiology, 85 (2012), e979–e986

Factors influencing the degree of enhancement of prostate cancer on contrast-enhanced transrectal ultrasonography: correlation with biopsy and radical prostatectomy specimens

[1]J JIANG, MD, [1]Y-Q CHEN, MD, [1]Y-K ZHU, MD, [2]X-H YAO, MM and [3]J QI, MD

[1]*Department of Ultrasound, Xinhua Hospital Affiliated to Shanghai Jiaotong University School of Medicine, Shanghai, China,* [2]*Department of Pathology, Xinhua Hospital Affiliated to Shanghai Jiaotong University School of Medicine, Shanghai, China, and* [3]*Department of Urology, Xinhua Hospital Affiliated to Shanghai Jiaotong University School of Medicine, Shanghai, China*

Objectives: This study was designed to identify factors that influenced the degree of enhancement of prostate cancer on contrast-enhanced transrectal ultrasonography (CETRUS).
Methods: 139 patients suspected of prostate cancer were evaluated with CETRUS followed by systematic and targeted transrectal ultrasound-guided biopsies. The degree of enhancement of the lesions was objectively measured using peak intensity with time–intensity curve analysis software. Ultrasound findings were correlated with clinical characteristics as well as biopsy and radical prostatectomy findings.
Results: Prostate cancers were detected in 230 biopsy sites from 91 patients. The mean peak intensity value of prostate cancer was significantly higher than that of the benign lesions (9.82 ± 3.73 *vs* 7.51 ± 2.97; $p<0.001$), and the peak intensity value of the cancer foci varied across the prostate. The mixed model analysis revealed that the location and Gleason score of tumour foci were the influencing factors of the peak intensity value, and the former had a stronger influence upon peak intensity than the latter ($p=0.000$ and 0.040, respectively). However, age, prostate volume or serum prostate-specific antigen of the patient had no significant influence on the peak intensity value ($p>0.05$). Furthermore, the peak intensity value of tumours larger than 5 mm diameter was significantly higher than tumours of 5 mm or smaller diameter (9.28 ± 2.46 *vs* 6.69 ± 2.65; $p<0.001$).
Conclusions: The prostate cancer lesions with a higher Gleason score and larger tumour size which were located in the lateral peripheral zone (PZ) were more likely to show a marked enhancement. Lesions with lower peak intensity that are located in the medial PZ should also be treated as suspicious.

Received 23 November 2011
Revised 28 February 2012
Accepted 12 March 2012

DOI: 10.1259/bjr/63794331

Prostate cancer is the most commonly diagnosed cancer in males, accounting for 28% of new cancer diagnoses in males and 11% of cancer-related deaths, with an expected 32 050 prostate cancer-specific mortalities in 2010 [1]. The imaging of prostate cancer is central to early detection and staging. However, it is generally acknowledged that detection and localisation of prostate tumours using greyscale ultrasound is poor, because suspicious hypoechoic areas represent cancer in only 9–53% of cases [2–3]. Furthermore, up to 30% of prostate cancers are isoechoic [4–5]. Conventional prostate ultrasound has little advantage over digital rectal examination for detecting malignant areas. Consequently, new strategies for prostate cancer detection are required. Contrast-enhanced ultrasound (CEUS) is a real-time imaging technique with the capability of visualising perfusion patterns [6–8]. This imaging technology has revealed promising perspectives in the diagnosis of prostate cancer owing to its ability to improve the visualisation of tumour vascularity. Several studies have reported that CEUS-targeted biopsy detected more cancer than systematic biopsy by identifying the area with greatest enhancement of the prostate [9–12]. In a recent study reported by Tang et al [13], the haemodynamic parameters such as time to enhancement (AT), time to peak intensity (TTP) and peak intensity (PI) were compared between 44 prostate cancer lesions and 47 benign ones. However, the peak enhancement intensity was found to be the optimal discriminatory parameter. Based on these previous findings, the degree of enhancement of the tumour foci plays a significant role in cancer detection on CEUS imaging.

Although CEUS detected more cases of cancer than baseline imaging, the cancer detection rate still remains far from satisfactory [14–15]. Halpern et al [14] compared

Address correspondence to: Dr Ya-qing Chen, Department of Ultrasound, Xinhua Hospital Affiliated to Shanghai Jiaotong University School of Medicine, 1665 Kongjiang Road, Shanghai 200092, China. E-mail: joychen_1266@163.com
The financial support from the Science and Technology Commission of Shanghai Municipality Foundation (09411963800, 10411952000, 10JC1411400) and Shanghai Jiaotong University School of Medicine Technology Foundation (11XJ21019) is gratefully acknowledged.

areas of increased enhancement in the prostate at CEUS with pathological examination and found that only 8 of 31 cancer foci were detected at baseline greyscale imaging, and contrast-enhanced imaging allowed identification of 13 of the 31 cancers (42% sensitivity). In their research, more than half of all cancers failed to show an abnormal enhancement, which indicated that the prostate cancer foci were not always shown as marked enhancement. Mitterberger et al [11] stated that the cancer with increased enhancement found by means of targeted biopsy had a higher mean Gleason score than the ones found by random biopsies, which suggested that the Gleason score of the prostate cancer could influence the degree of enhancement of the tumour to a certain extent. However, to our knowledge, factors influencing the degree of enhancement of the tumour have not yet been systematically investigated. In the present study, we evaluated the peak intensity of prostate cancers during the administration of the ultrasound contrast agent, and aimed to identify factors that influenced the degree of enhancement of prostate cancer on CEUS imaging. We hypothesised that identifying factors influencing the tumour peak intensity value could be useful for differential diagnosis of benign and malignant lesions in the CEUS examination, which would allow for a more accurate determination of the target sites during the subsequent biopsy procedure.

Methods and materials

Patients

A total of 139 consecutive male patients underwent contrast-enhanced transrectal ultrasonography, and subsequent transrectal ultrasound-guided prostate biopsies due to either abnormal digital rectal examination findings or abnormal serum prostate-specific antigen (PSA) levels ($\geq 4\,ng\,ml^{-1}$). 42 of 139 patients underwent prostatectomy following the diagnosis of prostate cancer. The study was approved by our local ethics committee, and written informed consent was obtained from all patients.

Imaging and biopsy protocol

Each patient was evaluated with ultrasound at baseline and again during intravenous bolus injection of SonoVue® (Bracco, Milan, Italy). The ultrasound equipment used was a Sequoia 512 with an EV8C4-S transrectal probe (Siemens Medical Solutions, Mountain View, CA). Normal greyscale imaging was performed with a probe frequency of 7.0 MHz and a dynamic range of 80 dB. For colour Doppler ultrasonography, the probe frequency was 6.0 MHz, and the colour Doppler gain was adjusted to maximise signal but eliminate colour noise from the tissue of the prostate. The colour Doppler window was set to include the entire gland. During CEUS examinations, a dose of 2.4 ml of SonoVue was infused intravenously followed by a 5 ml normal saline flush. The scanner was set in cadence contrast pulse sequencing (CPS) mode with a probe frequency of 8.0 MHz. The acoustic power was set at a mechanical index of 0.11 and the dynamic range was fixed at 81 dB. The CPS gain setting was set to automatic optimisation. The contrast imaging plane was chosen as the transverse plane of the sonographic abnormality, or the most hypervascular plane on colour Doppler imaging for patients with no suspicious findings on baseline ultrasonography. After the completion of ultrasound examination, all patients underwent both targeted and systematic ultrasound-guided prostate biopsies. First, the systemic 10-core biopsy was taken. The 10-core biopsy included eight cores obtained from the peripheral zone (PZ), consisting of the para-midline, the middle, the lateral and the anterior lateral horn part, as well as two cores from the transition zone (TZ). Then, up to four targeted biopsies were performed in patients with the abnormalities. All biopsy specimens were marked according to site of origin and placed in separate containers of 10% neutral buffered formalin. A map of the prostate whose shape and size were concordant with the contrast imaging plane was created during the biopsy procedure (Figure 1). For the purpose of marking the biopsy site, the prostate on the biopsy map was divided into PZ and TZ. The PZ gland was subdivided into medial gland and lateral gland. The TZ gland was subdivided into right and left sides. After the biopsy protocol, the biopsy site of each specimen was marked on this map. For the systemic biopsy cases, the para-midline biopsy site was marked in the medial gland region, while the biopsy sites of the middle, the lateral and the anterior lateral horn part were all documented in the lateral gland region. The two cores from TZ were marked in the right or left TZ region. In terms of the targeted biopsy protocol, each targeted biopsy site was assigned with the corresponding location according to its distribution on the biopsy map.

Pathological analysis

All the biopsy specimens for each case were analysed by a single pathologist who was expert in urological pathology and was not aware of the CEUS findings. The pathological findings were categorised as cancer, prostatic intra-epithelial neoplasia (PIN) or benign prostate hyperplasia (BPH) with or without inflammation.

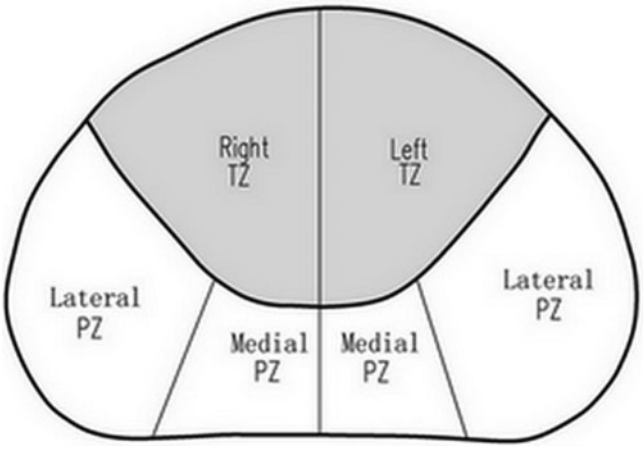

Figure 1. Biopsy map of the prostate used for marking the biopsy site. PZ, peripheral zone; TZ, transition zone.

Prostate cancers were assigned a Gleason score. Cancer foci with a Gleason score of 7 or more were categorised as high-grade tumours; the rest were categorised as low-grade tumours. The prostatectomy specimen was coated with India ink and fixed overnight in 10% formalin. The apex was cut into sagittal sections and the seminal vesicles were amputated separately. The remaining gland was serially sliced as whole mounts from the apex to the base at 4–5 mm intervals perpendicular to the long axis of the prostate. All the whole mounted specimen slices were photographed and printed as a histological map. Then, slices were submitted for paraffin embedding after being separated into two or four sections. Subsequently, microslices were placed on glass slides and stained with haematoxylin and eosin. An experienced pathologist reviewed all tissue sections, and the cancer areas were outlined on the previously printed histological map, along with tumour size (diameter) and Gleason score.

Image interpretation

All contrast-enhanced ultrasound data were saved in the workstation and analysed retrospectively using Axius™ ACQ software (TomTec, Fulda, Germany). On the contrast imaging plane, the regions of interest (ROIs) were identified through the biopsy maps created during the biopsy protocol, and the ROIs were drawn around the corresponding biopsy site, with a one-to-one correspondence between each ROI and biopsy site. The time–intensity curve was reconstructed for each ROI and then the peak intensity was generated, which shows the value of the maximum intensity in the ROI that occurs after time zero (in dB). During the evaluation of the haemodynamic data, observers were blinded to the pathological results, PSA values and other clinical information.

In the 42 prostatectomy specimens, the most closely corresponding transverse CEUS images and pathological step-section slices were paired on the basis of the following anatomical landmarks: (1) progressive changes in the diameter of the slices; (2) the slice where the ejaculatory ducts enter the verumontanum; (3) the anterior–posterior and left–right position of the urethra, and the shape of the urethra; (4) the thickness of the peripheral zone; and (5) the presence, size and shape of the transition zone. When the contrast image plane and corresponding pathological slice were matched, the ROI was drawn to fit the tumour foci on the histological maps as accurately as possible. Then the peak intensity of the cancer lesion could be obtained.

Statistical analysis

SPSS® v. 12.0 (SPSS Inc., Chicago, IL) was used for all statistical computations. Mixed-model analysis was used to obtain the influencing factor of peak intensity on CEUS findings among the clinical and histological characteristics such as age, prostate volume, PSA level, Gleason score and location. For the influencing factors that the mixed model revealed, stratification analysis with Student's *t*-test or one-way analysis of variance (ANOVA) was used to analyse the differences between the corresponding groups. In detail, if location was the influencing factor upon the peak intensity value, all lesions were first divided into medial PZ, lateral PZ and TZ groups, and then for each group the differences in peak intensity values between low- and high-grade cases were analysed. The correlation between the peak intensity of tumour foci and tumour size on prostatectomy specimen was calculated by Student's *t*-test analysis. Statistical data did not include the biopsy cores diagnosed as PIN because quantities were too small for statistical analysis: thus, only the prostate cancer and BPH lesions were analysed in the present study. $p<0.05$ was considered statistically significant, $p<0.01$ highly statistically significant and $p>0.05$ not statistically significant.

Results

Among 139 patients enrolled in this study, prostate biopsies revealed 91 patients with prostate cancer. The remaining 48 patients did not show cancer and were diagnosed with BPH. Among the prostate cancer patients, 42 underwent radical prostatectomy. For the patients with BPH, none had elevated serum PSA levels after a 1-year follow-up. The clinical characteristics of the patients are described in Table 1.

On histological examination, prostate cancer was identified in 230 (23.7%) of 969 biopsy specimens from 91 prostate cancer patients. BPH was diagnosed for all 501 biopsy cores generated from the 48 patients without cancer. Peak intensity values for 230 prostate cancer lesions and 501 BPH lesions are shown in Table 2. The mean peak intensity value in the prostate cancer samples was significantly ($p<0.001$) higher than that of the BPH lesions. There was a significant ($p<0.001$) difference between the degree of enhancement and tumour location between the prostate cancer group and the BPH group. After comparing the peak intensity of lesions between the benign and malignant groups in different locations, we found that the peak intensity values of prostate cancer lesions located in the medial and lateral PZs were significantly higher than those of the BPH lesions. However, lesions located in the TZ showed no statistically significant difference between the two groups (Table 2 and Figures 2–4).

Table 3 shows the clinical and histological characteristics of prostate cancer. To screen the factors that influenced peak intensity values, a mixed-model analysis was performed by using peak intensity as a dependent variable and location as a repeated variable. The results show statistically that the location and Gleason score of tumour foci were the influencing factors on the peak intensity value, and the former had a stronger influence upon peak intensity than the latter ($p=0.000$ and 0.040, respectively). However, age, prostate volume and serum PSA level of the patient had no significant influence on the peak intensity value ($p>0.05$).

After dividing the lesions into low- and high-grade tumour groups, statistical analysis revealed significant differences in peak intensity for different tumour locations in both groups ($p<0.001$) (Table 4). Specifically, peak intensity values for tumour lesions located in the TZ were highest and those for tumours in the lateral PZ were

Table 1. Clinical characteristics of patient groups

Characteristic	BPH	PCa	*p*-value
Number of patients	48	91	
Age [years, mean ± SD (range)]	67.53 ± 9.18 (45–83)	72.30 ± 6.85 (52–86)	<0.001
PSA [ng ml^{-1}, mean ± SD (range)]	6.90 ± 4.72 (0.3–15.1)	23.28 ± 24.40 (1–100)	<0.001
PSAD [ng ml^{-1} ml^{-1}, mean ± SD (range)]	0.21 ± 0.11 (0.01–0.56)	0.67 ± 0.76 (0.1–4.2)	<0.001

BPH, benign prostate hyperplasia; PCa, prostate cancer; PSA, prostate specific antigen; PSAD, PSA density; SD, standard deviation.
p-value obtained using the Mann–Whitney *U*-test.

secondary, whereas lesions in the medial PZ had, on average, the lowest peak intensity.

Table 5 demonstrates the peak intensity values of low- and high-grade tumours in the medial PZ, lateral PZ and TZ groups. Peak intensity values of low-grade tumours were lower than those of high-grade tumours in the medial PZ and lateral PZ groups ($p<0.001$). However, there was no statistically significant difference in the peak intensity value between low- and high-grade tumours located in the TZ ($p>0.05$).

By comparing the corresponding pathological step-section slices, 48 PZ and 18 TZ tumours were identified on the contrast image plane. Since the previous results showed that lesions located in the TZ had a completely different enhancement pattern than PZ lesions, we exclude the 18 TZ lesions when analysing the correlation between the peak intensity values and the size of the tumours. The 48 PZ tumours resulted in having 13 tumours ≤5 mm and 35 tumours >5 mm. Peak intensity values of tumours >5 mm were significantly higher than tumours ≤5 mm (9.28 ± 2.46 *vs* 6.69 ± 2.65; $p<0.001$).

Discussion

Prostate cancer tissue is associated with an increased microvessel density due to the proliferation of neovessels [16–18]. Since the parameter for peak intensity was defined as reflecting the blood volume in the ROIs [6], the development of neovascularity in the prostate cancer is demonstrated as increased peak intensity on CEUS imaging. Our data showed that the peak intensity of tumour foci was significantly higher than that of BPH lesions (9.82 ± 3.73 *vs* 7.51 ± 2.97, respectively; $p<0.001$). These results were consistent with the research in the literature and the pathological description about the tumour characteristics.

In our study, in addition to the observation that the peak intensity values were different between benign and malignant lesions, it also came to light that the degree of enhancement of the lesions differed significantly in various regions of the prostate in both the BPH and prostate cancer groups. In the BPH group, the peak intensity value of the lesions located in the TZ was highest, followed by that of the lateral PZ and finally the medial PZ. This phenomenon could be explained by the distribution of blood supply in different regions of the prostate. Previous studies have confirmed that BPH induces neovascularisation, and the main sources of blood supply of prostate are capsular vessels passing the urethra at the 1, 5, 7 and 11 o'clock positions, especially in the 5 and 7 o'clock positions. A large proportion of the capillaries run under the capsule, and then mostly run towards the urethra concentrically [19]. The TZ gland was the predilection site of BPH and had a rich blood supply, resulting in the highest enhancement on CEUS imaging. The lateral PZ gland also had an obvious contrast enhancement because of the adequate blood supply of capsular vessels, and the medial PZ gland had a weak enhancement because of poor blood supply and the pressure by BPH nodules in the TZ. Regarding the prostate cancer group, the peak intensity values of cancer foci in different locations showed the same trends as for BPH lesions. We then posed the following question: did the peak intensity values of cancer foci change according to only the distribution of blood supply of the prostate or were there any other factors that influenced the degree of enhancement of prostate cancer?

Table 2. Comparison of peak intensity between non-malignant lesions and prostate cancer lesions

Location	BPH (no. of lesions)	PCa (no. of lesions)	*p*-value
Medial PZ	4.52 ± 1.82 (101)	6.52 ± 2.80 (82)	<0.001
Lateral PZ	7.92 ± 2.75 (304)	10.56 ± 2.42 (96)	<0.001
TZ	13.67 ± 2.82 (96)	13.64 ± 2.36 (52)	>0.05
Total	7.51 ± 2.97 (501)	9.82 ± 3.73 (230)	<0.001

BPH, benign prostate hyperplasia; PCa, prostate cancer; PZ, peripheral zone; TZ, transition zone.
p-value obtained using the Student's *t*-test.

To solve this problem, we performed a mixed model to screen the influencing factors on the peak intensity value, and found that the location and Gleason score of the tumour foci could influence peak intensity values. To determine how tumour location and Gleason score influenced the peak intensity value of cancer foci, a stratified analysis was carried out by grouping the study sample according to tumour location or Gleason score. When the sample was divided into Gleason score subgroups, in neither the low-grade prostate nor in the high-grade prostate cancer was the variation trend of the tumour peak intensity the same as the BPH lesion, allowing us to assume that the peak intensity values of the tumours were affected by the distribution of blood supply in different regions of the prostate. Halpern et al [14] also found that the contrast enhancement was limited in the posterior midline segment of the PZ, and they supposed this phenomenon might be related to a probe pressure or a near-field effect. In our opinion, the lower peak intensity value of lesions located in the medial PZ was mainly due to the distribution of blood supply in different regions of the prostate. However, this conclusion requires further investigation for confirmation, as the number of prostatectomy cases in the present study was relatively low.

In the location subgroups, peak intensity values of low-grade tumours were lower than those of high-grade

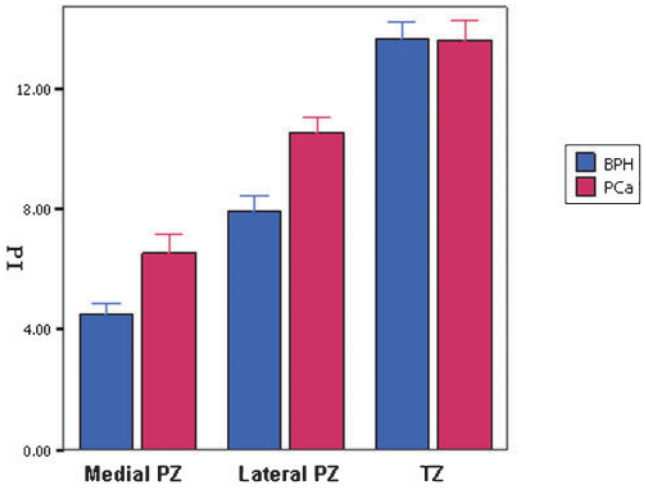

Figure 2. Peak intensity values of benign prostate hyperplasia (BPH) and prostate cancer (PCa) lesions located in medial peripheral zone (PZ), lateral PZ and transition zone (TZ).

tumours in the medial PZ and lateral PZ groups ($p<0.001$). Halpern et al [20] stated that higher-grade tumours tend to have increased microvessel density and should be easier to detect with contrast enhancement. This statement was in accordance with our present results. In another study performed in our institution [21], the relationship between peak intensity values and the Gleason score of prostate cancer was discussed. The authors evaluated the CEUS finding of 31 low-grade lesions and 123 high-grade lesions, and came to the same conclusion as we did: that the peak intensity value of high-grade PZ tumours was higher than that of low-grade PZ tumours. Mitterberger et al [10] also referred to the various enhancement of tumours assigned with different Gleason scores. They performed contrast-enhanced colour Doppler targeted biopsies plus 10-core systematic biopsies in 690 prostate-suspicious patients and found that the Gleason score of lesions with hypervascular enhancement was 6 or higher (mean 6.8), while the other lesions without abnormal enhancement ranged from 4 to 6 (mean 5.4). Although the haemodynamic parameter of the cancer lesions was not assessed in their research, the positive conclusion agrees with our study. However, in the TZ subgroup, there was no statistically significant difference in peak intensity values between the low- and high-grade tumours, nor between the BPH group and prostate cancer group. Deering et al [22] reported that the contrast-enhanced ultrasound was not helpful in the detection of cancers within the TZ gland. The difficulty with detection of TZ cancers is probably related to the intense, heterogeneous

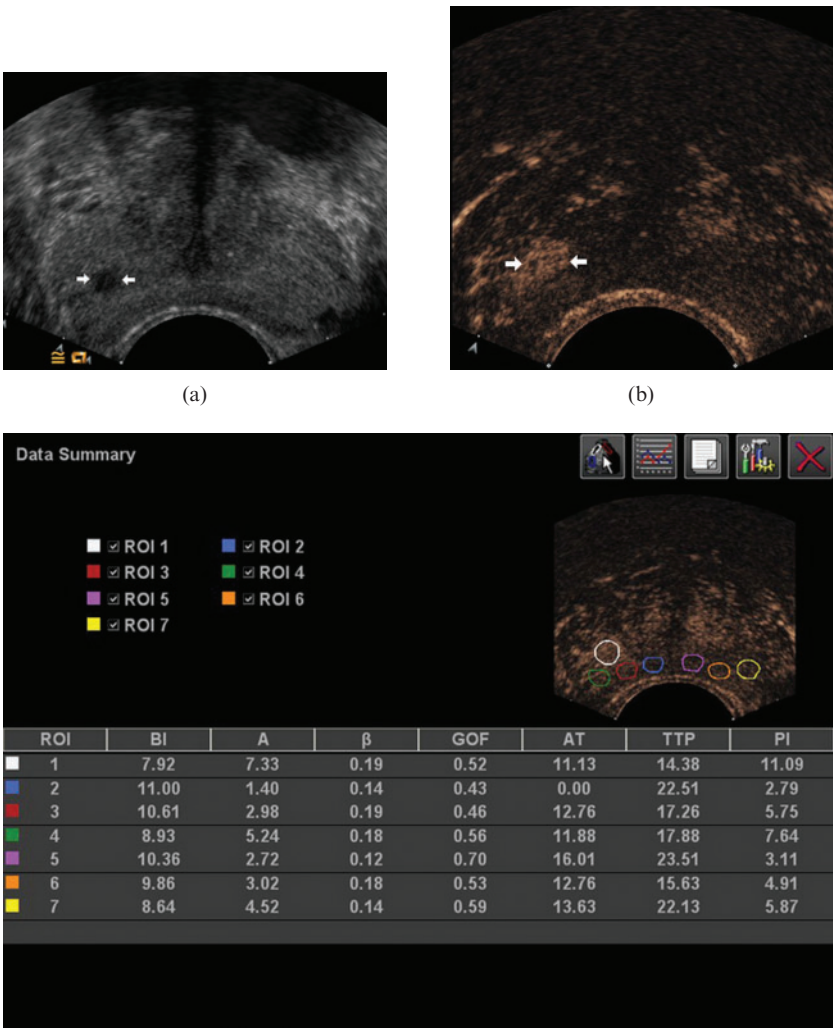

Figure 3. Ultrasound images in a 60-year-old male with Gleason 7 cancer at the right lateral peripheral zone of the prostate. (a) Conventional greyscale image demonstrated a focal hypoechoic lesion (arrows). (b) Contrast-enhanced image demonstrated a clearly defined area of focal enhancement, corresponding to the cancer (arrows). (c) On analysis with Axius™ ACQ software (TomTec, Fulda, Germany), the peak intensity of enhancement in this lesion was 11.09 dB (white circle).

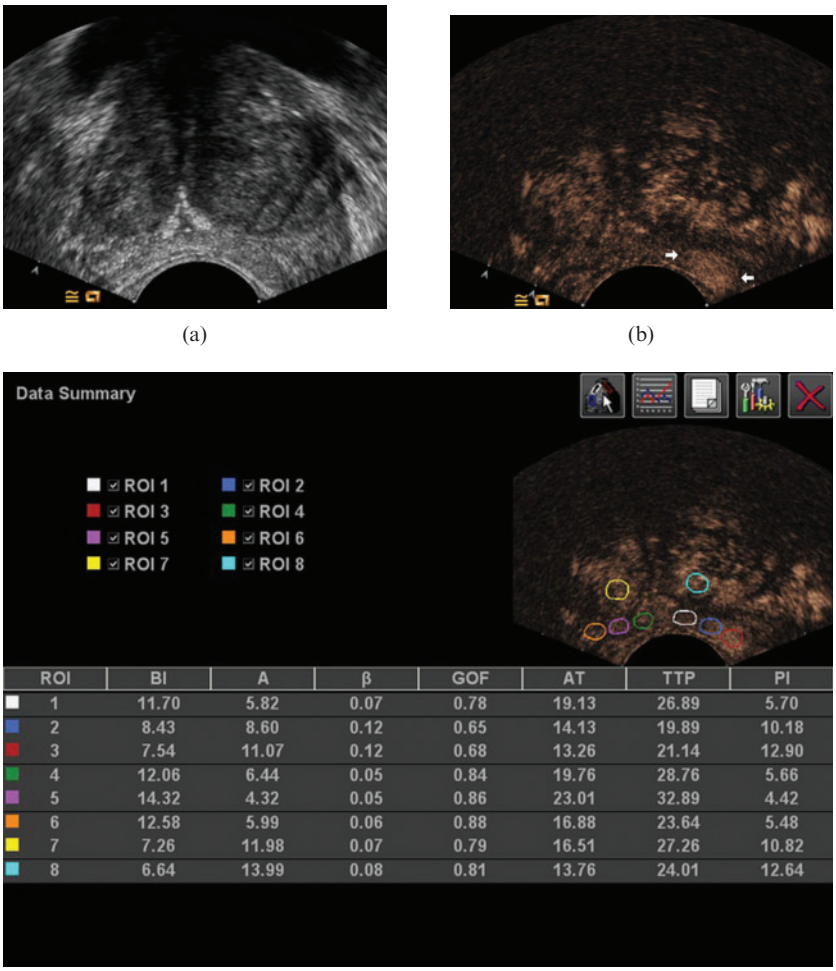

Figure 4. Ultrasound images in a 73-year-old male with Gleason 8 cancer, extending along the left peripheral zone from the medial part to the lateral part of the gland. (a) Conventional greyscale image demonstrated no definite lesion. (b) Contrast-enhanced image demonstrated focal enhancement in the left lateral gland (arrows). Although the tumour extended through the medial gland, no marked enhancement is seen in the medial peripheral zone. (c) On analysis with Axius™ ACQ software (TomTec, Fulda, Germany), the peak intensity values of cancer foci within the para-midline, the middle and the lateral biopsy site were 5.70 (white circle), 10.18 (blue circle), 12.90 (red circle), respectively.

enhancement pattern associated with benign prostatic hyperplasia. Since prostate cancer affects primarily older males, some degree of benign prostatic hyperplasia will be present in almost all subjects with cancer of the prostate [23].

In our study, the correlation between tumour size and the peak intensity value was also analysed by comparing the pathological step-section slices and the contrast image plane. The data showed that the peak intensity value of tumours with a diameter >5 mm was significantly higher than for tumours of ≤5 mm (9.28 ± 2.46 *vs* 6.69 ± 2.65; $p<0.001$). Renshaw [24] compared the gross findings and histological examination of 211 consecutive radical prostatectomy specimens and found that the larger tumours tended to be of higher grade and stage, whereas the grossly inapparent tumours (usually <5 mm) were often of a low grade and stage. Based on this research and the conclusions we previously obtained, that the low grade correlated with the lower enhancement, the present result of the smaller tumour focus in relation to lower peak intensity value could be explained. Sedelaar et al [12] performed three-dimensional contrast-enhanced power Doppler ultrasonography investigations on seven patients with biopsy-proven prostate cancer prior to radical prostatectomy. In their study, the prostate cancer lesions with an average maximum diameter of 25 mm (range 17–31 mm) showed an obvious enhancement, whereas the smaller cancer lesions (1–5 mm) were unidentifiable on the CEUS image. They also calculated the microvessel density (MVD) value of the prostate cancer, and found that larger tumours had a higher MVD count than benign prostate tissue, whereas small cancer foci showed no difference in MVD count compared with BPH. Based on their observations, we supposed that another possible

Table 3. Clinical and histological characteristics of patients with prostate cancer

Characteristic	Value	*p*-value
Age (years)	72.30 ± 6.85	0.491
Prostate volume (cm^3)	39.32 ± 18.64	0.564
PSA ($ng\,ml^{-1}$)	23.28 ± 24.40	0.719
Gleason score (no. of lesions)	230	0.040
Low grade	66	
6	66	
High grade	164	
7	101	
8	24	
9	39	
Location (no. of lesions)	230	<0.001
TZ	52	
Medial PZ	82	
Lateral PZ	96	

PSA, prostate specific antigen; PZ, peripheral zone; TZ, transition zone.
p-value obtained using mixed-model analysis.

Table 4. The peak intensity value of lesions with different locations in low- and high-grade tumour groups

Gleason score	Location	*n*	Peak intensity	*p*-value
Low-grade	Medial PZ	23	5.55 ± 1.99	
	Lateral PZ	31	9.82 ± 1.69	
	TZ	12	14.54 ± 0.94	
	Total	66	9.19 ± 3.60	<0.001
High-grade	Medial PZ	59	6.93 ± 3.00	
	Lateral PZ	65	10.91 ± 2.64	
	TZ	40	13.37 ± 2.59	
	Total	164	10.08 ± 3.75	<0.001

PZ, peripheral zone; TZ, transition zone.
p-value obtained using analysis of variance.

reason for lower peak intensity value in small tumours might be that the small prostate cancer lesions do not have an outspoken increased MVD when compared with large tumours, and consequently lead to a slight enhancement.

A limitation of the present study was difficulty with precise correspondence between the contrast image plane and the pathological slices. Because resection and fixation can result in deformation of the gland, and owing to the impossibility of sectioning identical planes with these two techniques, exact correspondence between pathological slices and the contrast image plane was not expected. However, a series of anatomical landmarks were used to pair the ultrasound image plane and the pathological slice as closely as possible. An additional limitation of our study was the relatively small study size of prostatectomy specimens.

Conclusions

The tumour location, Gleason score and tumour size were identified as the significant variables influencing the peak intensity values of prostate cancer lesions, while the age, PSA level and prostate volume had no correlation with the peak intensity value. Prostate foci with a higher Gleason score and larger tumour size and which were located in the lateral PZ were more likely to show a marked enhancement, which could then be easily recognised during a targeted biopsy procedure. Conversely, the peak intensity value of prostate cancer lesions with a lower Gleason score and smaller tumour size and which were located in the medial PZ tended to show weak enhancement or the same enhancement pattern as normal tissue on CEUS images. Therefore, lesions with lower peak intensity should still be treated as suspicious. Being aware of the factors influencing the degree of enhancement of the tumour may be valuable for differential diagnosis of prostate cancer from benign disease in the CEUS examination and localisation of the target sites in the subsequent biopsy procedure.

Table 5. The peak intensity value of low- and high-grade tumours in medial PZ, lateral PZ and TZ groups

Location	Gleason score	*n*	Peak intensity	*p*-value
Medial PZ	Low-grade	23	5.55 ± 1.99	
	High-grade	59	6.93 ± 3.00	
	Total	82	6.55 ± 2.81	0.045
Lateral PZ	Low-grade	31	9.82 ± 1.69	
	High-grade	65	10.91 ± 2.64	
	Total	96	10.56 ± 2.42	0.038
TZ	Low-grade	12	14.54 ± 0.94	
	High-grade	40	13.37 ± 2.59	
	Total	52	13.64 ± 2.36	0.135

PZ, peripheral zone; TZ, transition zone.
p-value obtained using Student's *t*-test.

References

1. Jemal A, Siegel R, Xu J, Ward E. Cancer statistics, 2010. CA Cancer J Clin 2010;60:277–300.
2. Pallwein L, Mitterberger M, Pelzer A, Bartsch G, Strasser H, Pinggera GM, et al. Ultrasound of prostate cancer: recent advances. Eur Radiol 2008;18:707–15.
3. Spencer JA, Alexander AA, Gomella L, Matteucci T, Goldberg BB. Clinical and US findings in prostate cancer: patients with normal prostate-specific antigen levels. Radiology 1993;189:389–93.
4. Mitterberger M, Horninger W, Aigner F, Pinggera GM, Steppan I, Rehder P, et al. Ultrasound of the prostate. Cancer Imaging 2010;10:40–8.
5. Halpern EJ, Strup SE. Using gray-scale and color and power Doppler sonography to detect prostatic cancer. AJR Am J Roentgenol 2000;174:623–7.
6. Cosgrove D. Ultrasound contrast agents: an overview. Eur J Radiol 2006;60:324–30.
7. Quaia E. Microbubble ultrasound contrast agents: an update. Eur Radiol 2007;17:1995–2008.
8. Matsumoto K, Nakagawa K, Hashiguchi A, Kono H, Kikuchi E, Nagata H, et al. Contrast-enhanced ultrasonography of the prostate with Sonazoid. Jpn J Clin Oncol 2010;40:1099–104.
9. Strohmeyer D, Frauscher F, Klauser A, Recheis W, Eibl G, Horninger W, et al. Contrast-enhanced transrectal color Doppler ultrasonography (TRCDUS) for assessment of angiogenesis in prostate cancer. Anticancer Res 2001;21:2907–13.
10. Mitterberger M, Horninger W, Pelzer A, Strasser H, Bartsch G, Moser P, et al. A prospective randomized trial comparing contrast-enhanced targeted versus systematic ultrasound guided biopsies: impact on prostate cancer detection. Prostate 2007;67:1537–42.
11. Mitterberger M, Pinggera GM, Horninger W, Bartsch G, Strasser H, Schafer G, et al. Comparison of contrast enhanced color Doppler targeted biopsy to conventional systematic biopsy: impact on Gleason score. J Urol 2007;178:464–8.
12. Sedelaar JP, van Leenders GJ, Hulsbergen-van de Kaa CA, van der Poel HG, van der Laak JA, Debruyne FM, et al. Microvessel density: correlation between contrast ultrasonography and histology of prostate cancer. Eur Urol 2001;40:285–93.
13. Tang J, Yang JC, Luo Y, Li J, Li Y, Shi H. Enhancement characteristics of benign and malignant focal peripheral nodules in the peripheral zone of the prostate gland studied using contrast-enhanced transrectal ultrasound. Clin Radiol 2008;63:1086–91.
14. Halpern EJ, McCue PA, Aksnes AK, Hagen EK, Frauscher F, Gomella LG. Contrast-enhanced US of the prostate with Sonazoid: comparison with whole-mount prostatectomy specimens in 12 patients. Radiology 2002;222:361–6.
15. Seitz M, Gratzke C, Schlenker B, Buchner A, Karl A, Roosen A, et al. Contrast-enhanced transrectal ultrasound (CE-TRUS) with cadence-contrast pulse sequence (CPS) technology for the identification of prostate cancer. Urol Oncol 2011;29:295–301.
16. Aigner F, Mitterberger M, Rehder P, Pallwein L, Junker D, Horninger W, et al. Status of transrectal ultrasound imaging of the prostate. J Endourol 2010;24:685–91.

17. Charlesworth PJ, Harris AL. Mechanisms of disease: angiogenesis in urologic malignancies. Nat Clin Pract Urol 2006;3:157–69.
18. Heijmink SW, van Moerkerk H, Kiemeney LA, Witjes JA, Frauscher F, Barentsz JO. A comparison of the diagnostic performance of systematic versus ultrasound-guided biopsies of prostate cancer. Eur Radiol 2006;16:927–38.
19. Slojewski M, Czerwinski F, Sikorski A. Microangiographic imaging of the prostate. BJU Int 2002;89:776–8.
20. Halpern EJ, Ramey JR, Strup SE, Frauscher F, McCue P, Gomella LG. Detection of prostate carcinoma with contrast-enhanced sonography using intermittent harmonic imaging. Cancer 2005;104:2373–83.
21. Zhu Y, Chen Y, Jiang J, Wang R, Zhou Y, Zhang H. Contrast-enhanced harmonic ultrasonography for the assessment of prostate cancer aggressiveness: a preliminary study. Korean J Radiol 2010;11:75–83.
22. Deering RE, Bigler SA, Brown M, Brawer MK. Microvascularity in benign prostate hyperplasia. Prostate 1995;26:111–15.
23. Eble JN, Sauter G, Epstein JI, Sesterhenn IA, editors. World Health Organization Classification of tumours: pathology and genetics of tumours of endocrine the urinary system and male genital organs. Lyon, France: IARC Press; 2004.
24. Renshaw AA. Correlation of gross morphologic features with histologic features in radical prostatectomy specimens. Am J Clin Pathol 1998;110:38–42.